ICSO 2016

International Conference on Space Optics

Biarritz, France

18–21 October 2016

Finite element model assisted shimming of Ingenio/Seosat primary mirrors

G. Taubmann

J. M. Arroyo

C. Miravet

D. Zorita

et al.

FINITE ELEMENT MODEL ASSISTED SHIMMING OF INGENIO/SEOSAT PRIMARY MIRRORS

G. Taubmann[1], J.M. Arroyo[1], C. Miravet[1], D. Zorita[1], C. Santos[1], I. Cabeza[2], A. Marini[3]

[1]SENER Ingeniería y Sistemas, c\Severo Ochoa 4, PTM, Tres Cantos, 28760 Madrid, Spain.
[2]AIRBUS Defence and Space, Avda. de Aragón 404, 28022 Madrid,Spain.
[3]ESTEC-ESA, postbus 299, Keplerlaan 1, 2200 AG Noordwijk,The Netherlands.

INTRODUCTION

Ingenio/SEOSAT is a multi-spectral high-resolution optical satellite for Earth remote sensing, designed to provide imagery to different Spanish civil, institutional and governmental users, and potentially to other European users in the frame of GMES and GEOSS. In this communication is presented the developed shimming procedure for the light-weighted primary mirror (M1) of the Ingenio/SEOSAT telescope, together with obtained results. The shimming operation has been devised to accurately cancel the residual deformation on the mirror surface caused by its integration on the telescope structure. This deformation is generally small but not necessarily negligible; even if all elements are integrated using proper isostatic mounts.

The devised shimming method uses as input a high-resolution deformation map of the M1 mirror surface, measured after mirror integration in the telescope structure. This map is obtained by a wavefront error measurement of the light reflected by the quasi-parabolic M1 mirror, placed on a null interferometric set-up. In the project, these interferometric measurements have been performed by REOSC-SAGEM, manufacturer of SEOSAT mirrors. The first 36 terms of the (fringe basis) Zernike decomposition of the measured surface deformation map have been computed and used in the shimming procedure.

The measured surface deformation maps can be modified by shimming the mirror support mounts, which induces its own deformation patterns. To quantify these contributions, a highly detailed finite element model (FEM) of the mirror and its interface mounting devices (IMDs) has been developed to characterize the mirror surface deformation map caused by unit displacements on each foot of the mirror support mounts. A Zernike decomposition of the resulting maps has then been performed, to enable a quantitative comparison to the results of the interferometric measurements. For the IMD configuration on Ingenio/SEOSAT M1 mirror, composed of three identical mounts located at 120 degrees around the mirror perimeter, the leading deformation pattern caused by mounting loads is primary astigmatism, with significantly smaller contributions to patterns such as primary trefoil and defocus.

The FEM analysis described enables to set up a set of linear equations relating IMD displacements to induced surface deformation Zernike coefficients. Solving these equations for the measured Zernike coefficients, one can get the set of IMD displacements that best reproduces the measured deformation map, in a least mean squared error sense. Applying these displacements with reverse sign using adequate shims, the mirror deformation can thus be optimally cancelled.

The use of this procedure on Ingenio/SEOSAT has enabled to reduce the initial residual astigmatism of the integrated primary mirror on a seventy five percent, with resulting performance even marginally better than that obtained at mirror manufacturing. The effect of shimming on telescope RMS wavefront error and modulation transfer function has been simulated, confirming the success of the approach. The presented approach has general applicability to the integration of a mirror of mid to large size, especially if its surface figure error has a critical impact on the overall image quality.

The devised procedure and obtained results are described in the following sections, preceded by a brief overview of the Ingenio/SEOSAT mission and payload.

SEOSAT MISSION OVERVIEW

Ingenio/SEOSAT [1-4] is a multi-spectral high-resolution optical satellite for Earth remote sensing, designed to provide imagery to different Spanish civil, institutional and governmental users, and potentially to other European users in the frame of GMES and GEOSS. Ingenio/SEOSAT is a Low Earth Orbiting mission. It features a Primary Payload (PP) with one 2.5 meter resolution panchromatic channel and four 10 meter

resolution visible/near infrared spectral channels. The PP swath close to 55 km ensures a frequent revisit period, and offers quick accessibility to any point on Earth in emergency situations.

Ingenio/SEOSAT is the flagship mission for the Spanish Space Plan elaborated by CDTI in 2006, and part of the Spanish Earth Observation Satellite System. This system comprises two spacecrafts with imagery capabilities in the optical and radar ranges, Ingenio/SEOSAT and Paz/SEOSAR, respectively. Following approval by ESA Council, an agreement was signed between the CDTI and the European Space Agency (ESA) concerning the technical and managerial assistance that ESA will provide to the Implementation phase of the Ingenio /SEOSAT Space and Ground Segment activities.

Ingenio/SEOSAT is designed for application in areas such as land use mapping, cartography, emergency support, water resources management, agriculture monitoring, environment, etc. The primary users, composed of several Spanish Governmental Organizations and Scientific Institutions, have defined the requirements of the mission, encompassing state-of-the-art image quality and radiometric performances. In order to fulfill these requirements, it has been defined a high performance instrument, facing several engineering challenges in both design and manufacturing terms.

Fig. 1. Artist's view of the Ingenio/SEOSAT satellite

SEOSAT PRIMARY PAYLOAD

A 3D view of the payload is presented in fig. 2. The payload is equipped with two identical cameras, each covering half of the requested image swath. Following the light path, each camera is composed of the following elements:

- An optical telescope based on an all-reflective Korsch concept.

- A focal plane assembly composed of two panchromatic (PAN) plus two multispectral (MS) detectors, co-planarly located. Detectors for both channels are of CCD type. The detectors used for the PAN channel are based on Time Delay and Integration (TDI) technology to increase the number of generated photo-electrons, with the corresponding improvement in signal-to-noise ratio. A 4-line CCD detector has been used for the MS channel, with lines devoted to sense blue, green, red and NIR spectral bands. Both PAN and MS detectors are mounted on its proper sub-assembly, which includes the filters defining the spectral bands and the corresponding proximity electronics.

- The electronics modules, including the electronic video units, the video power supply and the interface and control electronics.

Fig. 2. 3D view of the Ingenio/SEOSAT primary payload

The optical layout of the designed Korsch-type telescope is displayed in fig. 3. The system is composed of three conical on-axis mirrors (M1-M3) plus a plane folding mirror (FM) to direct the image to the focal plane (FP), in the upper part of the drawing. This design presents a high mechanical compactness, and maintains a relative ease of both manufacturing and alignment.

The designed system is all-reflective but for filters and windows located at the focal plane, and hence is essentially free of chromatic aberrations. This is particularly convenient given the extended spectral range of the instrument, spanning from blue to near infrared.

The larger mirrors in the design, M1 and M3, have been light-weighted to reduce the telescope mass. This contributes to the necessity of controlling the state of surface deformation during integration of M1, specially, given its large effect on the telescope overall wavefront error.
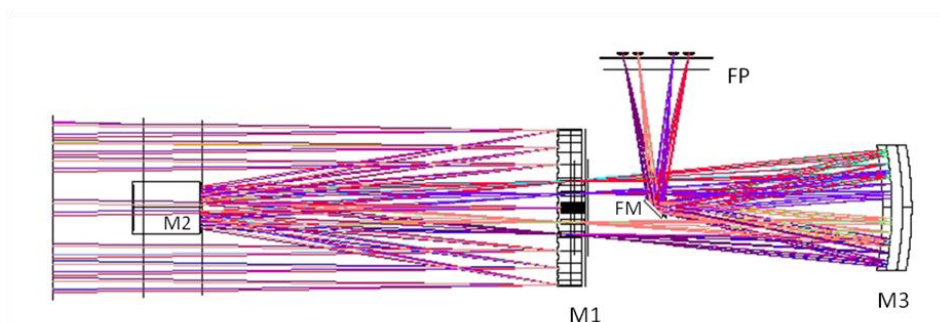

Fig. 3. Telescope optical design layout. Incoming light (from the left in the drawing) is focused on the focal plane (FP) after reflections on the primary (M1), secondary (M2), tertiary (M3) and plane folding (FM) mirrors

PRIMARY MIRROR FEM-ASSISTED SHIMMING MODEL

Ingenio/SEOSAT primary mirror (M1) is manufactured in Zerodur, a SCHOTT glass-ceramic well known for its extremely low thermal expansion coefficient. In fig. 4 is depicted a 3D model of the mirror, where it is apparent the light-weighting design in the mirror back, and the iso-static three-mount system at 120°. The IMDs are manufactured using a combination of Invar and Titanium. Invar (displayed in green in the figure) is used in the area that is glued to the M1 body, to minimize differential thermal expansion stresses induced in the mirror.

The structural part of the IMD (displayed in cyan) is manufactured using Titanium, with better performances due to a better rate elasticity modulus vs mass and larger micro-yielding strength.
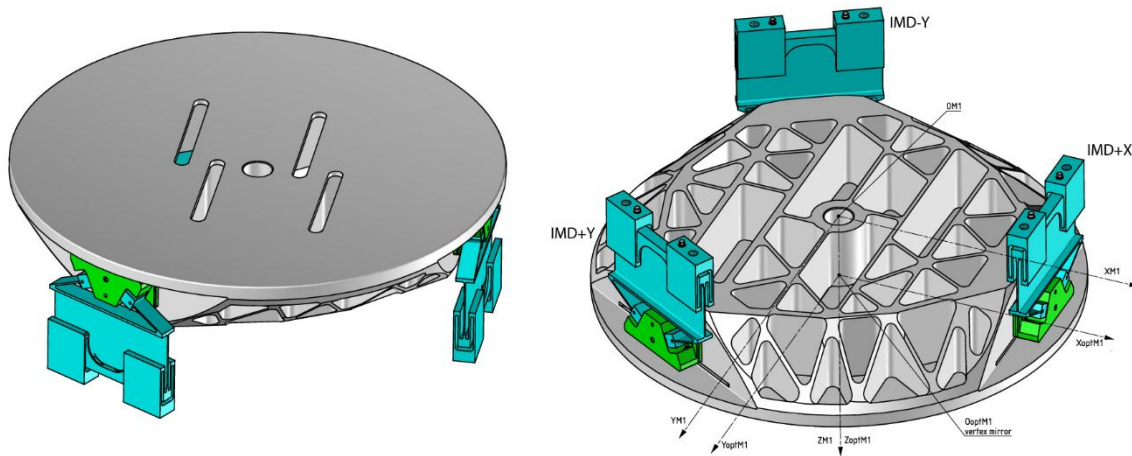

Fig. 4. Primary mirror mechanical model (courtesy of REOSC-SAGEM)

These IMDs provide a direct mechanical interface to a plane surface on the telescope structure. Each mounting device has two independent rectangular contact surfaces, which could be shimmed independently. Shimming both surfaces by the same amount induces a pure translation of the mounting device. Contrariwise, shimming both surfaces by opposite amounts induces mainly a rotation. In fig. 5 are presented the computed mirror surface deformation maps for unitary translations (first row) and rotations (second row) of each of the three IMDs. A unitary translation is defined here as corresponding to the displacement of both IMD contact surfaces by one micron in the same direction. In the same way, a unitary rotation corresponds to the relative displacement of both IMD contact surfaces by one micron. IMDs have been labelled as +X (first column), +Y (second column) and −Y (third column) in accordance to the IMD location with respect to the mirror reference frame (see fig. 4, right panel).
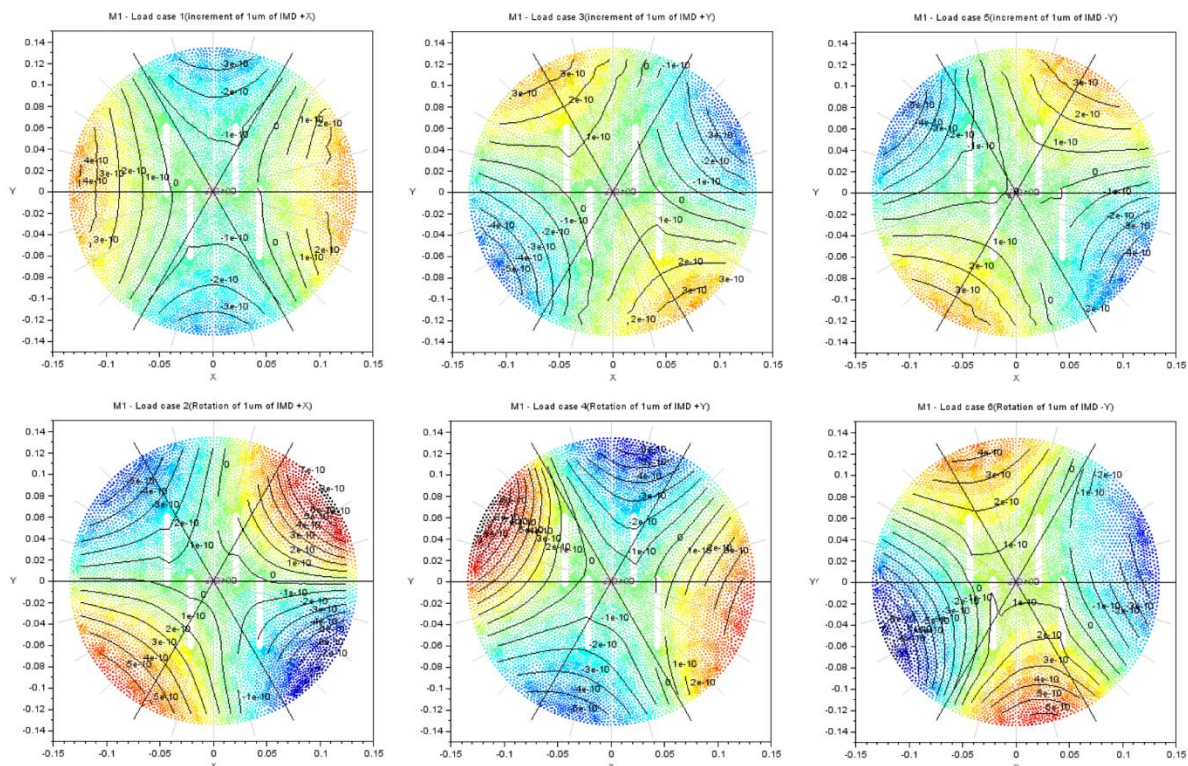

Fig. 5. Computed M1 surface deformation maps for unitary translations and rotations on each M1 IMDs
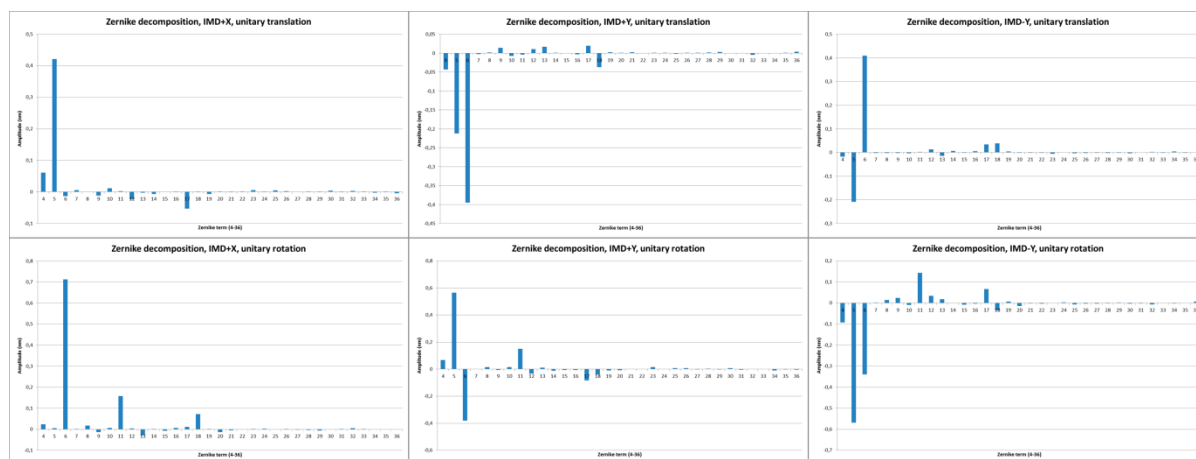
Fig. 6. Zernike decomposition of the unitary mirror surface deformation maps

Assuming a linear behavior of the mirror, the knowledge of the surface deformation due to unitary shims, allows predicting the deformation due to any shim combination by a simple arithmetic operation. In the same way, it is easy to evaluate the shim combination needed to obtain a determined surface shape.

In fig. 6 are displayed the first 36 coefficients of the Zernike decomposition of the computed surface deformation maps, piston and tilts excluded. As it is apparent, the leading deformation pattern induced by shimming in this geometry is primary astigmatism, described by coefficients Z_5 (horizontal-vertical axis) and Z_6 (axis at ±45°). Primary trefoil, particularly in the y-axis (Z_{11}) and defocus (Z_4) are also present, in significantly smaller magnitudes. Very minor contributions to other patterns, such as primary tetrafoil (Z_{17}-Z_{18}) and secondary astigmatism (Z_{12}-Z_{13}), have also been revealed by the study. The leading role of astigmatism is also apparent in the deformation maps depicted in fig.5, which show in all cases an astigmatic-like pattern.

Hence, we can conclude that the basic deformation pattern induced by IMD shimming on this mirror/IMD geometry is primary astigmatism, regardless of which IMD it is acted upon, or whether it has been subjected to translation or rotation. According to this, the effective number of degrees of freedom of the shimming operation is reduced from six to two, corresponding to the magnitude and orientation of the astigmatism pattern. These two degrees of freedom could be obtained by shimming in any two IMDs, applying translation or rotation displacements, as long as both unitary deformation maps are not oriented in the same orientation, or in orientations multiple of 90°.

Shimming resulting in IMD rotations has been discarded, as the FEM analysis showed it to create higher internal stresses than that consisting of IMD translations, for the same induced mirror surface deformation map. Considering only translations, three IMD pairs are possible: (+X, +Y), (+X, -Y) and (+Y, -Y). Use of any of the first two combinations is feasible, whereas elements of the third pair have deformation patterns roughly oriented at 90° with respect to each other. Use of this last pair will require considerable larger shims that the first two to generate horizontal-vertical astigmatism patterns, and thus its use has been discarded. The first two pairs are basically equivalent. The described implementation has used pair (+X, +Y).

M1 SHIMMING RESULTS

In the following paragraphs are presented the shimming results for the primary mirror on the payload's first telescope, including mirror surface deformation maps before and after shimming, determined shimming values and predicted effect of shimming on the mirror surface error and telescope wavefront error.

M1 initial surface deformation map
In fig. 6 is displayed the measured surface deformation map (left panel), with its low order map (mid panel) and high frequency residual (right panel). The low order map has been computed as the sum of the first 36 terms in the fringe Zernike decomposition. The high-frequency residual is the remainder obtained from subtracting the low order map from the measured map. In table I are presented the numerical values of coefficients Z_5 and Z_6 in the Zernike (fringe) decomposition, corresponding to horizontal-vertical and diagonal primary astigmatism, respectively.

Table I. Primary astigmatism Zernike coefficients before shimming

#Zern	Term	Value
Z_5	Primary astigmatism (axis at 0º, -90º)	9.4 nm
Z_6	Primary astigmatism (axis at +45º, -45º)	23.8 nm

The relatively large value of diagonal astigmatism causes the appearance of a diagonal pattern in the surface deformation map, clearly visible in both the total and low order maps. This degradation could be significantly reduced by application of the described shimming procedure.
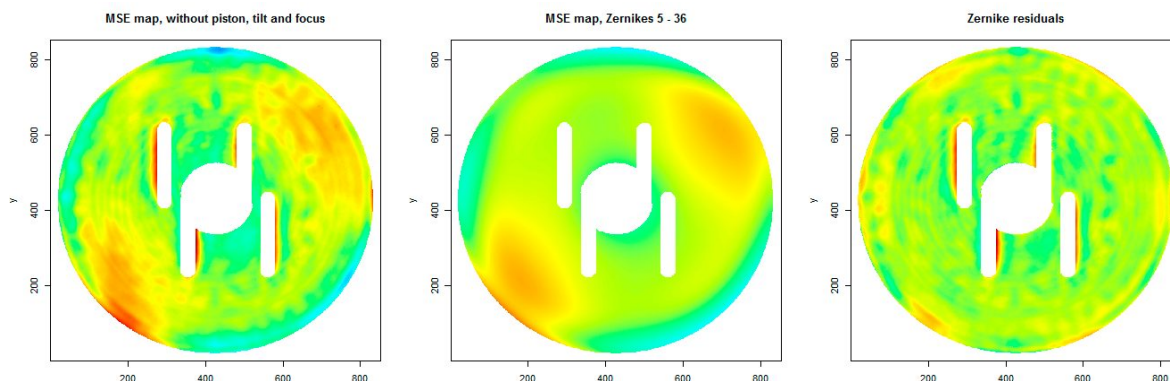

Fig. 7. M1 surface deformation map, before application of the shimming procedure

Shim thickness computation

Cancellation of the measured (low order) surface deformation map requires computing the solution to the following set of linear equations:

$$\alpha_i S_x + \beta_i S_y = -Z_i, \quad i = 5 \cdots 36, \tag{1}$$

with one equation per computed low order Zernike, up to Z_{36}. Piston, tilt and focus (Z_{1-4}) are excluded from the analysis. S_x and S_y represent here the thickness of the shims to be applied on IMDs +X and +Y, respectively. Coefficients α_i and β_i, linking shim thickness to induced surface deformation Zernike coefficients have been obtained directly from the performed FEM analysis, and are represented graphically in fig. 6. Finally, Z_i stands for the *i* measured Zernike coefficient, in the fringe basis. The sign of the measurement is inverted, to look for shimming solutions that cancel the observed deformation pattern.

This system of equations is highly overdetermined, with 32 equations for two unknowns. The least mean squared error solution can be determined by means of the Moore-Penrose pseudoinverse, which can be readily computed using singular value decomposition (SVD). In practical terms, the shimming solution will be basically determined by the cancellation of the astigmatism coefficients, which are the ones most largely affected by shimming (see fig. 6).

Application of this procedure have resulted in the shim thickness values presented in table II, after rounding to the nearest integer multiple of 5 µm. Shimming with these values was applied to M1, with the result described in the following paragraphs.

Table II. Shim thickness applied in IMD+X and IMD+Y

IMD	Shim thickness
+X	5 µm
+Y	55 µm

M1 surface deformation map after shimming
As for the case before shimming, in fig. 8 is displayed the total surface deformation map (left panel), low order map (mid panel) and high frequency residual. In table II are presented the numerical values of coefficients Z_5 and Z_6 in the resulting Zernike decomposition.

Table III. Primary astigmatism Zernike coefficients after shimming

#Zern	Term	Value
Z_5	Primary astigmatism (axis at 0º, -90º)	1.9 nm
Z_6	Primary astigmatism (axis at +45º, -45º)	-6.2 nm

The quadratic sum of these coefficients is $\sqrt{1.9^2 + (-6.2)^2} = 6.5\ nm$, a mere 25% of the corresponding value before shimming. In the low order map of figure 6, it can be seen that the diagonal pattern has been largely diminished, also experiencing a rotation of 90º (linked to the change of sign in Z_6).
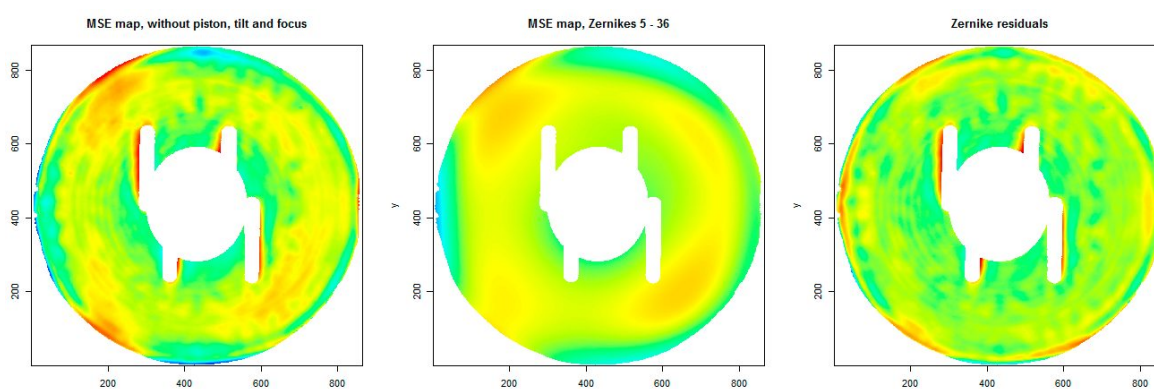

Figure 8. M1 surface deformation map, after shimming

Telescope wavefront error and modulation transfer function prediction

In table IV is presented the predicted effect of the performed shimming operation on both the telescope root mean squared wavefront error (WFE RMS) and on the polychromatic MTF at Nyquist frequency, for six fields (P1-P6) in the panchromatic channel of the instrument. Computation of these values have been performed using CODE V optical design program on SEOSAT's nominal optical design, with all mirrors equipped with their measured surface deformation maps.

According to this data, application of the described M1 shimming procedure results in a general improvement in the optical quality of the telescope, quantified both in terms of WFE RMS and MTF in X/Y directions. The expected peak WFE RMS decrease is close to 9 nm. For MTF, maximum increases of almost 14% are predicted. Both these improvements are considered to be highly relevant in terms of resulting optical performance, confirming the success of the proposed approach.

Table IV. Predicted telescope image performance parameters

	Results before shimming					
	P1	P2	P3	P4	P5	P6
WFE RMS (nm)	38.5	37.8	32.8	34.0	32.1	37.8
MTF X	0.252	0.261	0.291	0.281	0.290	0.276
MTF Y	0.240	0.250	0.271	0.269	0.265	0.247
	Results after shimming					
	P1	P2	P3	P4	P5	P6
WFE RMS (nm)	31.8	29.1	24.2	25.4	27.1	34.7
MTF X	0.284	0.297	0.311	0.304	0.303	0.282
MTF Y	0.27	0.282	0.292	0.292	0.279	0.26

CONCLUSIONS

A FEM based shimming method developed in the framework of SEOSAT project has been presented. The presented approach has general applicability to the integration of a mirror of mid to large size, especially if its surface figure error has a critical impact on the overall image quality.

Application of this procedure on Ingenio/SEOSAT has enabled to reduce the initial residual astigmatism of the integrated primary mirror on a seventy five percent, with resulting performance even marginally better than that obtained at mirror manufacturing. The effect of shimming on telescope RMS wavefront error and modulation transfer function has been simulated, confirming the success of the approach.

REFERENCES

[1] A. Marini, F.J. Reina Barragan, G. Crippa, B. Harnisch *et al*., "SEOSAT/INGENIO - A SPANISH HIGH-SPATIAL-RESOLUTION OPTICAL MISSION", *International Conference on Space Optics(ICSO)*, CNES-ESA, October 2014.

[2] C. Miravet, D. Zorita, J.I. Bueno, L. Pascual *et al*. "Development status of the telescope for the Ingenio/SEOSAT mission primary payload", *Proc. SPIE 8167, Optical Design and Engineering IV*, September 2011.

[3] L. Pascual, J.I. Bueno, D. Zorita, C. Miravet *et al*., "Detailed Optical Design of SEOSAT/Ingenio Spanish High Resolution Imaging Instrument", *International Conference on Space Optics(ICSO)*, CNES-ESA, October 2012.

[4] D. Zorita, C. Miravet, J.I. Bueno, "Challenges and developed solutions for the principal payload of the SEOSAT/Ingenio mission", *RAQRS III, Recent Advances in Quantitative Remote Sensing*, September 2010.